Developmental Biology 405 (2015) 237–249

Contents lists available at ScienceDirect

Developmental Biology

journal homepage: www.elsevier.com/locate/developmentalbiology

# PKA-dependent phosphorylation of LIMK1 and Cofilin is essential for mouse sperm acrosomal exocytosis

Ana Romarowski [a], María A. Battistone [a], Florenza A. La Spina [a], Lis del C. Puga Molina [a], Guillermina M. Luque [a], Alejandra M. Vitale [a], Patricia S. Cuasnicu [a], Pablo E. Visconti [b], Darío Krapf [c], Mariano G. Buffone [a,*]

[a] Instituto de Biología y Medicina Experimental (IBYME), Consejo Nacional de Investigaciones Científicas y Técnicas (CONICET), Buenos Aires, Argentina
[b] Department of Veterinary and Animal Science, Paige Labs, University of Massachusets, Amherst, MA 01003, USA
[c] Instituto de Biología Molecular y Celular de Rosario (CONICET-UNR), Rosario 2000 Argentina

ARTICLE INFO

*Article history:*
Received 6 January 2015
Received in revised form
1 July 2015
Accepted 9 July 2015
Available online 10 July 2015

*Keywords:*
Small GTPases
Acrosomal exocytosis
Actin
Cofilin
LIMK1
Sperm

ABSTRACT

Mammalian sperm must acquire their fertilizing ability after a series of biochemical modifications in the female reproductive tract collectively called capacitation to undergo acrosomal exocytosis, a process that is essential for fertilization. Actin dynamics play a central role in controlling the process of exocytosis in somatic cells as well as in sperm from several mammalian species. In somatic cells, small GTPases of the Rho family are widely known as master regulators of actin dynamics. However, the role of these proteins in sperm has not been studied in detail. In the present work we characterized the participation of small GTPases of the Rho family in the signaling pathway that leads to actin polymerization during mouse sperm capacitation. We observed that most of the proteins of this signaling cascade and their effector proteins are expressed in mouse sperm. The activation of the signaling pathways of cAMP/PKA, RhoA/C and Rac1 is essential for LIMK1 activation by phosphorylation on Threonine 508. Serine 3 of Cofilin is phosphorylated by LIMK1 during capacitation in a transiently manner. Inhibition of LIMK1 by specific inhibitors (BMS-3) resulted in lower levels of actin polymerization during capacitation and a dramatic decrease in the percentage of sperm that undergo acrosomal exocytosis. Thus, we demonstrated for the first time that the master regulators of actin dynamics in somatic cells are present and active in mouse sperm. Combining the results of our present study with other results from the literature, we have proposed a working model regarding how LIMK1 and Cofilin control acrosomal exocytosis in mouse sperm.
© 2015 Elsevier Inc. All rights reserved.

## 1. Introduction

Mammalian sperm are not able to fertilize eggs immediately after ejaculation. They must undergo a series of biochemical modifications in the female reproductive tract collectively called capacitation (Austin, 1951; Chang, 1951). Capacitation prepares the sperm to develop two main features that are essential for fertilization to occur: the capacity to develop hyperactivated motility and the acquisition of the ability to undergo a secretory event known as acrosomal exocytosis. Men or mice carrying mutations affecting the process of acrosomal exocytosis are infertile or display some degree of subfertility (Dam et al., 2007; Kang-Decker et al., 2001; Lin et al., 2007). To penetrate the zona pellucida (ZP), the extracellular matrix surrounding the egg, mammalian sperm must undergo acrosomal exocytosis in an orderly manner (Buffone et al., 2009; Yanagimachi, 1994). In addition, only acrosome-reacted sperm are able to relocalize Izumo1, a protein essential for sperm egg-fusion, to the equatorial segment (Miranda et al., 2009).

One important unresolved question regarding acrosomal exocytosis is how capacitation triggers the priming of the acrosome for exocytosis. Following the tethering/docking of the outer acrosomal membrane and the plasma membrane, the fusion machinery needs to be assembled for exocytosis to occur (Mayorga et al., 2007). Many groups have identified proteins in sperm that have been previously described to participate in exocytosis of secretory cells, such as Rab3A, the SNARE family, α-SNAP, NSF, complexin, the calcium-binding protein synaptotagmin, calmodulin and dynamin among others (De Blas et al., 2005; Hutt et al., 2005; Michaut et al., 2001; Rodríguez et al., 2011; Roggero et al., 2007; Tomes et al., 2005; Yunes et al., 2002; Zhao et al., 2007). In addition, it was recently shown that membrane hyperpolarization that occurs during capacitation is necessary and sufficient to prepare the sperm to undergo acrosomal exocytosis upon appropriate

* Corresponding author.
*E-mail address:* mgbuffone@ibyme.conicet.gov.ar (M.G. Buffone).

http://dx.doi.org/10.1016/j.ydbio.2015.07.008
0012-1606/© 2015 Elsevier Inc. All rights reserved.

stimuli (De La Vega-Beltran et al., 2012). However, how a change in membrane potential or other molecular events that prepare the sperm to undergo exocytosis interplay during capacitation are still unknown. One possible mechanism that could coordinate different aspects of cell signaling in sperm is the regulation of the actin cytoskeleton. In somatic cells, actin dynamics play a central role in controlling the processes of exo/endocytosis (Porat-Shliom et al., 2013). In several mammalian species, actin polymerization occurs during sperm capacitation (Brener et al., 2003; Cabello-Agüeros et al., 2003; Hernández-González et al., 2000). In addition, polymerized actin filaments (F-actin) have been proposed to be severed prior to acrosomal exocytosis (Cabello-Agüeros et al., 2003; Finkelstein et al., 2010; Spungin et al., 1995). The polymerization of F-actin during capacitation occurs not only in the sperm head but also in the flagellum (Itach et al., 2012). The capacitation induced-actin polymerization that takes place in the sperm head may play a role in stabilizing the fusogenic structures observed during capacitation. In other systems, the cortical actin network acts as a dominant negative clamp that blocks constitutive exocytosis (Muallem et al., 1995). Nemoto et al. (2004) revealed that newly fused granules in pancreatic acinar cells are rapidly coated with F-actin which slows the rate of granule fusion without reducing the overall extent of exocytosis. Thus, F-actin stabilizes structures generated by exocytosis and supports the physiological progression of this event.

Sperm actin polymerization was reported to depend on phospholipase D (PLD) activity and regulated by cross-talk between protein kinases A (PKA) and C (PKC) (Cohen et al., 2004). In somatic cells, small GTPases of the Rho family are widely known as master regulators of actin dynamics. However, the role of these proteins in sperm has not been studied in detail. In mammals, the Rho family is composed by the small GTPases Rho, Rac and Cdc42 which switch between an active GTP-bound and an inactive GDP-bound form. The cycling of Rho GTPases between these two states is regulated by three sets of proteins: guanine nucleotide exchange factors (GEFs), GTPase activating proteins (GAPs) and guanine nucleotide dissociation inhibitors (GDIs). Some reports have shown the presence of small GTPases in mammalian sperm (Baltiérrez-Hoyos et al., 2012; Ducummon and Berger, 2006; Fiedler et al., 2008; Freeman et al., 2002). In guinea pig sperm, it was suggested that small GTPases RhoA, RhoB and Cdc42 may participate in acrosomal exocytosis (Delgado-Buenrostro et al., 2005). However, their function in mature mouse sperm remains mostly unknown.

Small GTPases activate downstream effector proteins when bound to GTP, thereby stimulating a variety of cellular processes such as morphogenesis, migration, vesicle transport, actin dynamics, etc. Interestingly, the activation of Rho, Rac and Cdc42 and the subsequent signal transduction through specific downstream effectors results in the phosphorylation of LIM-kinases (LIMKs; composed of LIMK1 and LIMK2 in mammals) (Amano et al., 2001; Ohashi et al., 2000). In turn, the phosphorylation of LIMKs results in the activation of Cofilin (Bernstein and Bamburg, 2010). Cofilin is a family of actin-binding proteins that regulate assembly and disassembly of actin filaments. The activity of Cofilin is regulated by several mechanisms, of which phosphorylation has been best characterized. LIMKs specifically phosphorylate Cofilin at Ser-3 and thereby inhibit the actin binding, severing, and depolymerizing activities of Cofilin. Thus, protein kinases and phosphatases related to Cofilin phosphorylation and dephosphorylation at Ser-3 are expected to play a central role in the regulation of actin dynamics.

In the present work, we describe and characterize for the first time the participation of small GTPases of the Rho family in the signaling pathway that leads to actin polymerization during mouse sperm capacitation. We found that modulation of LIMK1 and Cofilin by phosphorylation is essential for controlling the process of capacitation-induced actin polymerization and acrosomal exocytosis.

## 2. Materials and methods

### 2.1. Reagents

Chemicals were obtained from the following sources: bovine serum albumin (BSA), progesterone, TRITC-labeled phalloidin, and calcium ionophore A23187 were purchased from Sigma (St. Louis, MO); membrane-permeable Exoenzyme C3 Transferase (C4) was obtained from Cytoskeleton (Denver, CO); Y-27632 was acquired from Cayman Chemicals (Ann Arbor, MI); InSolution RAC1 inhibitor (CAS 1177865-17-6) and H89 from Calbiochem; IPA-3, dbcAMP and IBMX from Sigma and BMS-3 from SynKinase; Anti-phosphotyrosine (pY) monoclonal antibody (clone 4G10) was obtained from Upstate Biotechnology (Lake Placid, NY); anti-RHOA, anti-RHOB, anti-RHOC, anti-ROCK, anti-PAK1, anti-LIMK1, anti-LIMK2, anti-Cofilin, anti-phospho-LIMK1/2 (pLIMK1/2) and anti-phospho- Cofilin (pCofilin) antibodies were purchased from Cell Signaling (Danvers, MA); Anti-β-Tubulin monoclonal antibody was obtained from Sigma. Anti-RAC1 and anti-ACTIN antibodies and propidium iodide were purchased from Santa Cruz (Santa Cruz, CA); Horseradish peroxidase-conjugated anti-mouse and anti-rabbit IgG were purchased from Vector and Cell Signaling respectively.

### 2.2. Animals

HybridF1 (C57BL/6xBalb/C) mature (10–12 week-old) male mice, as well as mature transgenic [BDF1-Tg (CAG- mtDsRed2, Acr-EGFP) RBGS0020sb] male mice who have sperm with acrosomal vesicles expressing green EGFP fluorescence and midpieces (mitochondria) expressing red Ds-Red2 fluorescence (Hasuwa et al., 2010), were used. Animals were maintained at 23 °C with a 12 h light: 12 h dark cycle. Animal experimental procedures were reviewed and approved by the Ethical Committee of IBYME (CE/003-1/2011). Experiments were performed in strict accordance with the Guide for Care and Use of Laboratory Animals approved by the National Institutes of Health (NIH).

### 2.3. Sperm capacitation

In all the experiments, mouse sperm were recovered by incising the caudae epididymides in 500 μl of a modified Krebs-Ringer medium (Whitten's-HEPES-buffered (WH) medium) (Moore et al., 1994). This medium, which does not support capacitation, was prepared without bovine serum albumin (BSA) and $NaHCO_3$. After 10 min of incubation at 37 °C, epididymides were removed, and sperm were resuspended to a final maximum concentration of $1 \times 10^7$ cells/ml in the appropriate medium depending on the experiment performed. For capacitation, a medium without HEPES containing 5 mg/ml of BSA and 15 mM of $NaHCO_3$ was used, and sperm incubated at 37 °C in an atmosphere of 5% $CO_2$ in air. The pH was maintained at 7.4. To test the effect of inhibitors on capacitation, sperm were pre-incubated with inhibitors in non-capacitating medium for 10 min prior to the beginning of the capacitating period.

### 2.4. Extraction of sperm proteins

Sperm were collected by centrifugation for 5 min at 3000 rpm, washed (5 min, 10,000 rpm) in 1 ml of PBS, resuspended in sample buffer (62.5 mM Tris–HCl pH 6.8, 2% SDS, 10% v/v glycerol) and

boiled for 4 min. After centrifugation for 5 min at 13,000 rpm, 5% ß-mercaptoethanol was added to the supernatants and boiled again for 4 min. Bromophenol blue was added to a final concentration of 0.0005% to the mixture. Protein extracts equivalent to $2–5 \times 10^6$ sperm per lane were separated by SDS-PAGE and immunoblotted.

### 2.5. Extraction of Triton-insoluble sperm proteins

Sperm were collected by centrifugation for 5 min at 3000 rpm, washed (5 min, 10,000 rpm) in 1 ml of PBS, resuspended in 30 μl of extraction buffer (Tris 50 mM, NaCl 150 mM, 1% Triton X-100, 0.1% SDS and protease and metalloprotease inhibitor mixture [Thermo Scientific], pH 7.8) and vortexed vigorously (15 s). The sperm extracted protein suspension was placed on ice for 10 min. The sample was then centrifuged at 13,000 rpm (13,600*g*) for 5 min at 4 °C. The Triton-insoluble (I) content of the protein sample was obtained by removing the supernatant fluid (Triton-soluble content, (S)) from the pellet, which was resuspended with 40 μl of sample buffer. The 30 μl of Triton-soluble content was mixed with 10 μl of sample buffer 4X. Both fractions were boiled for 4 min. After centrifugation of the Triton-insoluble content for 5 min at 13,600*g*, 5% ß-mercaptoethanol was added to the supernatant and to the Triton-soluble extract and both were boiled again for 4 min. Bromophenol blue was added to both mixtures at a final concentration of 0.0005%. Triton-soluble and Triton-insoluble protein extracts were obtained from $6 \times 10^6$ sperm and were separated by SDS-PAGE and immunoblotted.

### 2.6. Immunoblotting

The proteins were separated by SDS-PAGE in gels containing 10% or 15% polyacrilamide according to the method of Laemmli (1970) and transferred onto nitrocellulose membranes (Towbin et al., 1979). Blots were blocked in 5% nonfat dry milk in PBS containing 0.1% Tween 20 (T-PBS) for 1 h at room temperature and incubated for an over night at 4 °C with the first antibody. Antibodies were diluted in 2% nonfat dry milk in T-PBS as follows: 1:500 for anti-PAK1 and anti-pLIMK1/2, 1:100 for anti-RhoA, B, C, anti-LIMK1, anti-LIMK2, anti-pCofilin, anti-Cofilin and for anti-ACTIN and 1:200 for anti-Rac1. The corresponding secondary antibodies were diluted in 2% nonfat dry milk in T-PBS as follows: 1:1000 for anti-rabbit and 1:4000 for anti-mouse. For anti-pY (1:3000) and anti-ß-Tubulin (1:7000) immunodetections, first and secondary antibodies were diluted in T-PBS. In all the cases the reactive bands were detected by enhanced chemiluminescence (GE Healthcare, Piscataway, NJ, USA). When necessary, membranes were stripped for 10 min in 2% SDS, 0.67% ß-mercaptoethanol, 62.5 mM Tris pH 6.8. In all experiments, molecular masses were expressed in kilodaltons. As a loading control, phosphoHexokinase (pHKS) (constitutively phosphorylated on tyrosine and detected with anti-pY antibody) (Kalab et al., 1994) or anti-ß-Tubulin was used. For band quantification, rectangular boxes were drawn around bands on scanned digital images of ECL contact photographs of western blots, and adjusted optical densities for each lane were obtained using ImageJ software 1.47 V (National Institute of Health, USA).

### 2.7. Immunofluorescence

To perform Immunofluorescence on mouse sperm, we used a previously described method (Sosnik et al., 2010). Briefly, mouse sperm obtained from caudae epididymides and capacitated for different times were washed twice by centrifugation for 5 min at 3000 rpm, resuspended in PBS, and placed onto glass slides. Sperm were air-dried and then treated with PBS containing 4% formaldehyde for 15 min at room temperature. After washing twice for 5 min in T-PBS, sperm were permeabilized with 0.5% Triton X-100 in PBS for 5 min. The slides were then washed twice for 5 min and incubated in T-PBS containing 10% normal goat serum (blocking buffer) for 1 h at room temperature, then with primary antibody (1:100 for anti-pLIMK1/2 and anti-pCOFILIN and 1:50 for COFILIN) diluted in T-PBS containing 1% normal goat serum for an overnight at 4 °C. Following a washing step (three times, 5 min in T-PBS), slides were incubated with FITC-conjugated goat anti-rabbit IgG diluted 1:200 in T-PBS containing 1% normal goat serum for 1 h at room temperature, washed again for three times, and mounted using Vectashield (Vector Labs, Burlingame, CA, USA). Nonspecific staining was determined by incubating the sperm with rabbit IgG. Slides were examined using a laser scanning confocal microscope (Nikon C1 Eclipse 800; Nikon Corporation) and images were captured at 40× magnification, N.A=0.9 (air).

### 2.8. Fluorescence staining of actin filaments

Cells were fixed in 0.1% glutaraldehyde and 1.5% formaldehyde in PBS for 1 h and collected by centrifugation at 4000 rpm for 5 min. The sperm pellet was immediately resuspended and incubated with 50 mM $NH_4Cl$ in PBS during 15 min and washed twice by resuspension/centrifugation in PBS and once in distilled water. Water-resuspended cells were used to prepare smears, which were air dried at room temperature for an overnight. Smears were rinsed with PBS for 7 min and then permeabilized using acetone at −20 °C for 7 min, and washed three times in PBS. Slides were then incubated with 50 μl TRITC-phalloidin (1:30) in PBS, under cover glass slides for 1 h at room temperature in humid conditions, in the dark. Smears were washed three times with PBS, once in distilled water and air-dried at room temperature. For observation, they were mounted under cover glass slides using Vectashield. Slides were examined using a laser scanning confocal microscope Nikon C1 Eclipse 800 and images were captured at 40× magnification, N.A=0.9 (air). The fluorescence intensity was quantified using ImageJ software 1.47 V (National Institute of Health, USA). The intensity of fluorescence was calculated in regions of interest localized in the sperm head. The background intensity was subtracted.

### 2.9. Determination of actin incorporation into the Triton-insoluble cytoskeleton of sperm

The actin content of the Triton-insoluble fraction (F-actin) was assessed as detailed above (Section 2.5) by removing the supernatant (Triton-soluble G-actin) from the pellet. The extracted proteins were separated by SDS-PAGE and immunoblotted with anti-actin antibody (1:100).

### 2.10. Acrosomal exocytosis using flow cytometry

Acrosomal exocytosis was assessed as previously described (Muro et al., 2012; Hirohashi et al., 2015). Briefly, Acr-EGFP mouse sperm were incubated under capacitating conditions for 90 min in the presence or absence of increasing concentrations of pLIMK inhibitor BMS-3. After 90 min, progesterone (20 or 50 μM) or calcium ionophore A23187 (10 μM) were added for 30 min to stimulate the acrosomal exocytosis. The EGFP sperm were analyzed on a flow cytometer (FACSCanto II flow cytometer, BD) to evaluate acrosomal status after adding propidium iodide to the sperm suspension to determine the sperm viability. A (515–545) nm band path filter and 650 nm long path filters were used for GFP and propidium iodide, respectively.

### 2.11. Statistical analysis

Data are expressed as mean ± SEM of at least three experiments for all determinations. Statistical analyses were performed using ANOVA and a Tukey's multiple comparisons test using the GraphPad Prism 6 software (La Jolla, CA USA). Statistical significance is indicated in the figure legends.

## 3. Results

### 3.1. Capacitation-induced actin polymerization

Actin polymerization during sperm capacitation has been postulated as an essential requisite for acrosomal exocytosis (Brener et al., 2003). First, we evaluated the normal time course of actin polymerization during mouse sperm capacitation. Sperm were lysed in a detergent-based lysis buffer that stabilizes and maintains the G- and F-forms of cellular actin. Because the buffer solubilizes G-actin but does not solubilize F-actin, it was possible to separate G- and F-actin by centrifugation (F-actin in the pellet and the G-actin in the supernatant). As depicted in Fig. 1A, the amount of F-actin increased after 90 min of capacitation while the levels of G-actin (soluble) decreased due to its incorporation into the F-actin fraction. The increase in actin polymerization occurred as rapid as 15 min after sperm were incubated in capacitating conditions (Fig. 1B). The formation of F-actin was also visualized by phalloidin–TRITC staining (Fig. 1C). The increase in F-actin content was observed in the head as well as in the flagellum. Actin polymerization was quantified at different times by measuring the fluorescence intensity in the sperm head. As shown in Fig. 1D, phalloidin staining increased as early as 15 min of incubation in

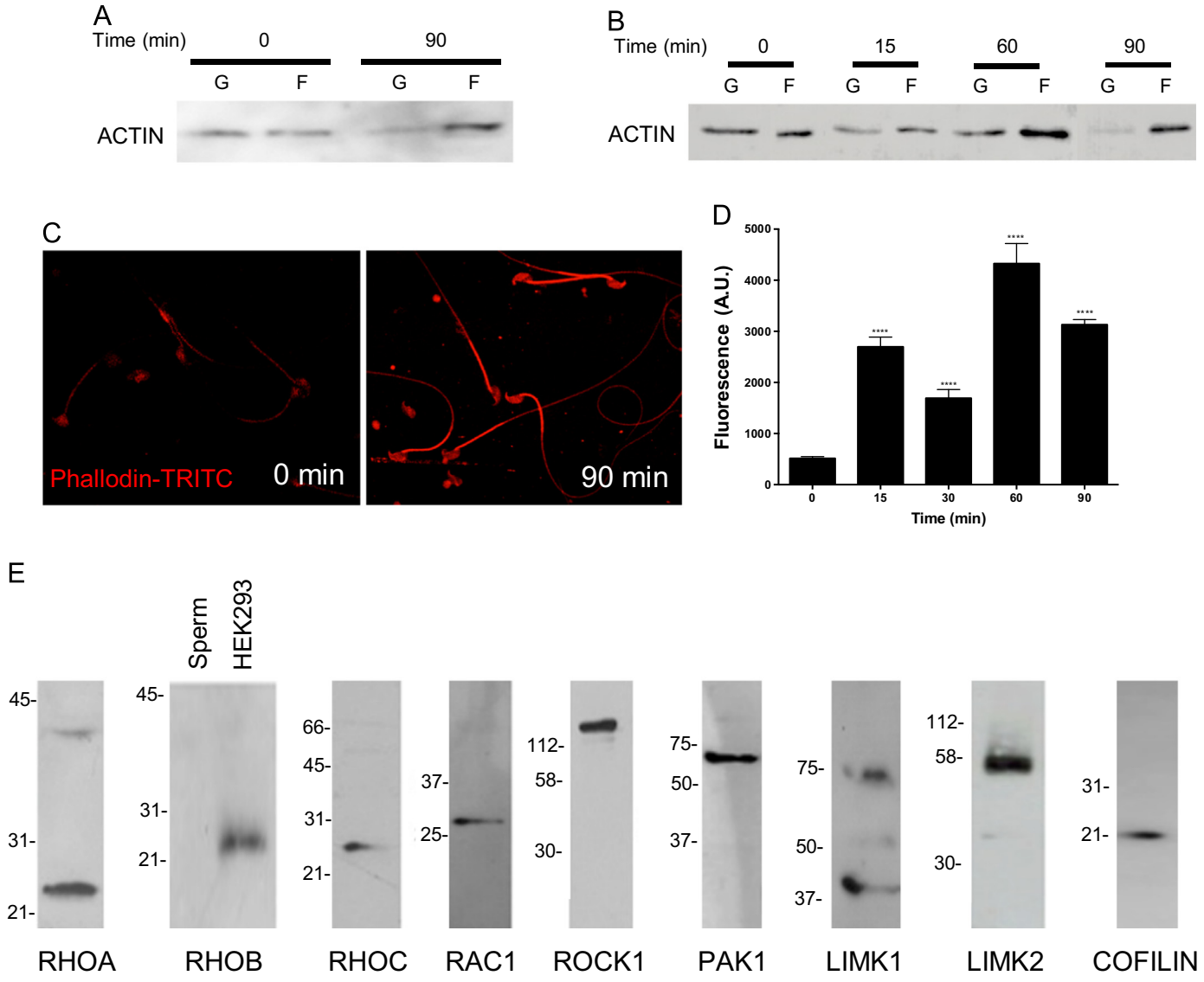


**Fig. 1.** *All the components of the RHO/RAC pathway leading to actin polymerization are present in mature mouse sperm.* (A) Mouse sperm were incubated for 90 min under capacitating conditions. The F-actin and G-actin contents at the beginning and end of this incubation were determined by immunoblotting. (B) Mouse sperm were incubated for up to 90 min under capacitating conditions. At the indicated time points, the G- and F-actin content was determined by immunoblotting. (C) Fluorescent staining of actin filaments. Representative images of sperm stained by TRITC-phalloidin before and after capacitation. (D) Quantitative analysis of the fluorescence intensity after staining with TRITC-phalloidin at different time points of the incubation under capacitating conditions. Results are expressed as the mean ± SEM of 3 independent experiments. ****represents significant difference compared with 0 min ($P < 0.0001$). A.U. denotes arbitrary units. (E) Mouse sperm proteins were analyzed by 10–15% SDS-PAGE and immunoblotted using antibodies against the small GTPases RHOA, RHOB, RHOC, RAC1 and the effector proteins ROCK1, PAK1, LIMK1, LIMK2 and COFILIN. In the experiments for RHOB (protein was not detected) HEK293 cells were run in parallel as appropriate controls. Each lane contained 2–5 × $10^6$ sperm except for LIMK1 (protein equivalent to 40 × $10^6$ sperm was loaded).

capacitation supporting media (Fig. 1D). It was also noticeable that the F-actin formation in the sperm head did not increase steadily. Instead, an oscillation in the F-actin content was observed between 15 and 30 min of incubation.

### 3.2. Small GTPases and their effector proteins are expressed in mouse sperm

Small GTPases of the Rho family regulate actin dynamics in somatic cells. Although different members of the Rho family have been shown to be expressed in sperm from other species, only Cdc42 has been reported in mouse. We hypothesized that these proteins may also play a role in sperm. To test this hypothesis, we evaluated the presence of proteins belonging to the Rho family of small GTPases as well as of some of their effector proteins known to be involved on actin polymerization. Within the Rho family, only Cdc42 was shown to be present in mature mouse sperm (Baltiérrez-Hoyos et al., 2012). As shown in Fig. 1E, sperm extracts also contained RhoA, RhoC and Rac1, but not RhoB. We also detected the effector proteins ROCK1, PAK1, LIMK1, LIMK2 (only the testis-specific isoform of 52,000 $M_r$) and Cofilin in mature sperm at the expected molecular weights. These results indicate that all the necessary components for an active signaling pathway leading to actin polymerization are present in mouse sperm.

### 3.3. LIMK1 Is phosphorylated on Thr508 during capacitation

In other cell types different effector proteins are stimulated upon activation of Rho, Rac and Cdc42. In the case of RhoA/C, the effector protein is Rock1, whereas for Rac and Cdc42, the effector protein is the kinase PAK1-4. In turn, both ROCK1 and PAK1 phosphorylate and activate LIMK1 (on Thr508) and LIMK2 (on Thr505). Our results showed that after 90 min of in vitro capacitation, LIMK1 was phosphorylated on Thr508 (Fig. 2A). This phosphorylation was already detected as early as 10 min of incubation under capacitating conditions (Fig. 2B). Phosphorylated LIMK1 (pLIMK1) was only detected in the Triton-insoluble fraction (Fig. 2B). The molecular weight of LIMK1 is 70,000 $M_r$. In the case of LIMK2, there is a testis-specific isoform of 52,000 $M_r$ (Takahashi et al., 2002). Because of the molecular weight of the phosphorylated form of LIMK (72,000 $M_r$), we conclude that in mouse sperm, LIMK1 and not LIMK2 is phosphorylated on Thr508 during mouse sperm capacitation. As shown in Fig. 2C phosphorylated LIMK1 (pLIMK1) was detected in the middle piece of the sperm flagellum as well as in the acrosomal cap.

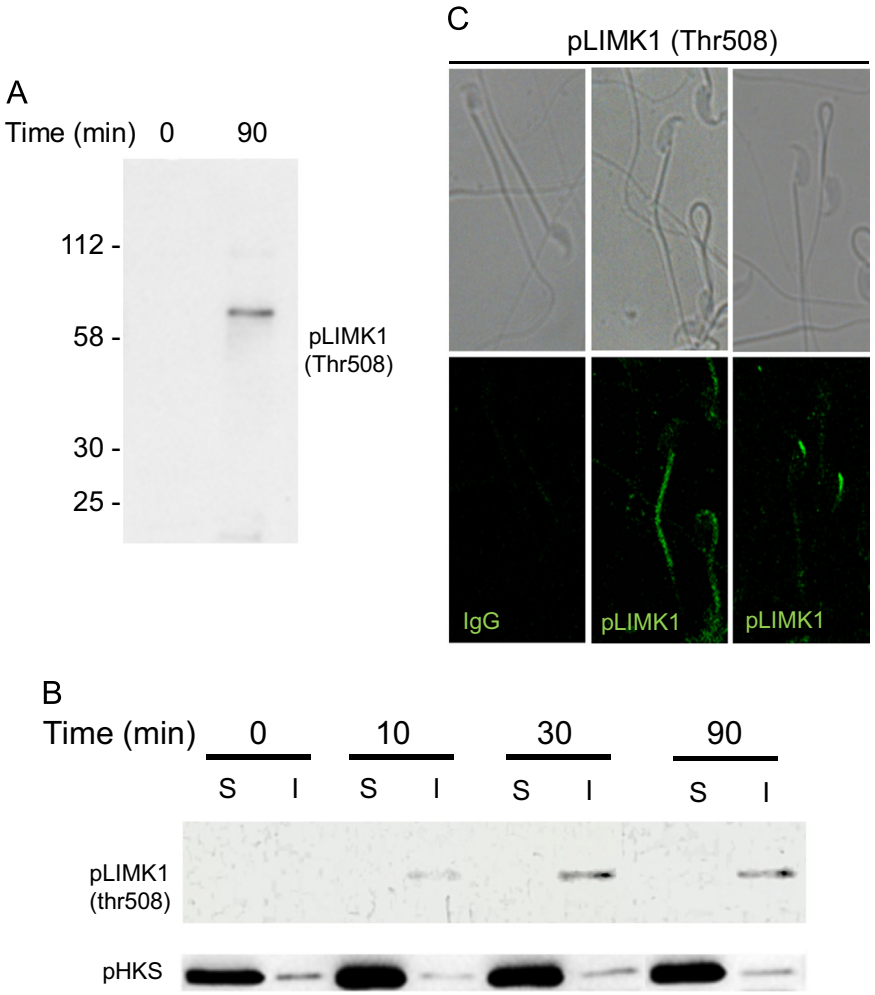


**Fig. 2.** *LIMK1 is phosphorylated on Thr 508 during capacitation.* (A) Mouse sperm were incubated for 90 min under capacitating conditions. The protein extracts were analyzed by 10% SDS-PAGE and immunoblotted with anti-phosphoLIMK1/2 (Thr508/505) antibody. (B) Mouse sperm were incubated for up to 90 min under capacitating conditions. At the indicated times, the Triton-soluble (S) and Triton-insoluble (I) content of the protein extract were analyzed by 10% SDS-PAGE and immunoblotted with anti-phosphoLIMK1/2 (Thr508/505) antibody. As a loading control, phosphoHexokinase (pHKS) (constitutively phosphorylated on tyrosine) was used. Each lane contained $5 \times 10^6$ sperm. (C) Immunofluorescence showing the localization of pLIMK1 (Thr508) in the sperm middle piece and in the acrosomal region after 90 min of incubation in capacitating conditions. Top panels correspond to the bright field images of the fluorescence panels shown at the bottom. Negative control was performed incubating the sperm with IgG. Representative images of 4 independent experiments.

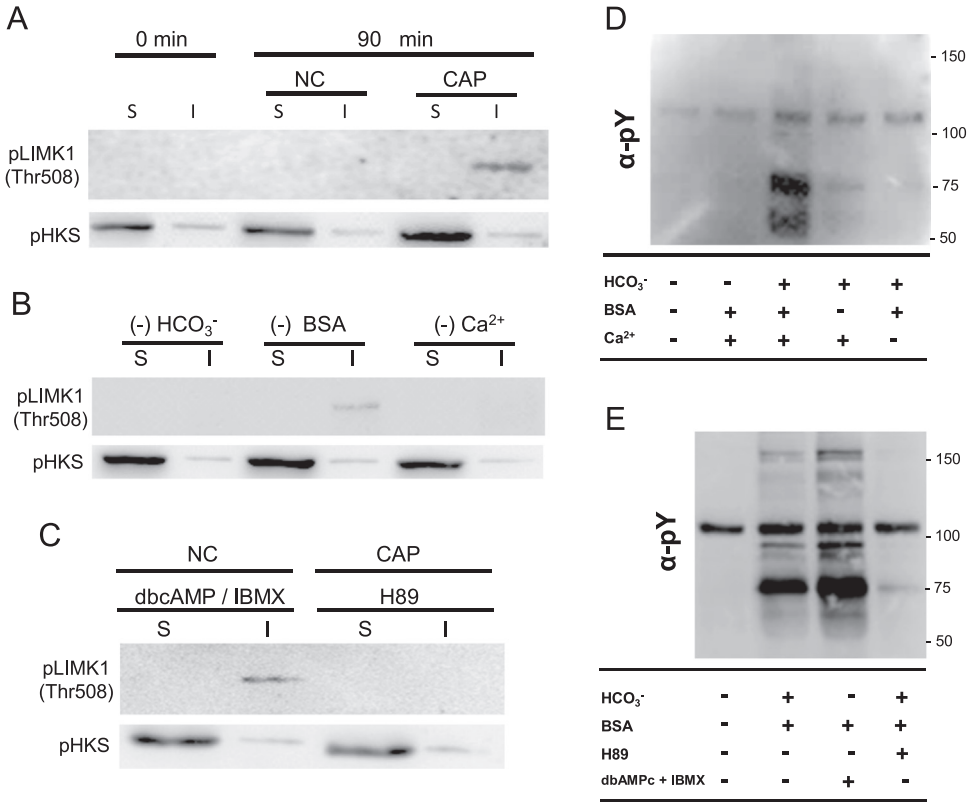


**Fig. 3.** *LIMK1 phosphorylation on Thr 508 is dramatically decreased under non-capacitating condition or in the presence of inhibitors of PKA, suggesting that this process is strongly associated with capacitation.* Sperm were incubated under different conditions for 90 min. The Triton-soluble (S) and Triton-insoluble (I) content of the protein extract were analyzed by 10% SDS-PAGE and immunoblotted with anti-phosphoLIMK1/2 (Thr508/505) antibody. As a loading control, phosphoHexokinase (pHKS) (constitutively phosphorylated on tyrosine) was used. Each lane contains $5 \times 10^6$ sperm. (A) Capacitating (CAP) or non-capacitating (NC: media lacking BSA and $HCO_3^-$) conditions. (B) Incubation in media lacking $HCO_3^-$, BSA or $Ca^{2+}$ separately. (C) Under non-capacitating conditions with the addition of dbcAMP/IBMX (1 mM and 0.2 mM, respectively) or in capacitating conditions in the presence of 30 μM H89. (D) As a control, a fraction of the samples used in A and B were used to detect anti-phospho-tyrosine (pY). (E) As a control, a fraction of the samples used in C was used to detect anti-phospho-tyrosine (pY). Representative images of 5 independent experiments.

### *3.4. The activation of the signaling pathways of cAMP/PKA, RhoA/C and Rac1 are essential for LIMK1 phosphorylation*

The presence of $Ca^{2+}$, BSA and $HCO_3^-$ in the culture medium is essential for the onset of phosphorylation events associated with capacitation (Visconti et al., 1995). Moreover, our previous data suggested that LIMK1 is activated by threonine phosphorylation during capacitation. To investigate the signaling pathways that lead to phosphorylation of LIMK1, we performed experiments omitting these critical components in the culture medium. LIMK1 was not phosphorylated in the absence of BSA and $HCO_3^-$ (Non-capacitating conditions; NC) (Fig. 3A). When these components were omitted separately, no phosphorylation was observed either, except for the medium lacking BSA, where reduced levels of pLIMK1 were noted (Fig. 3B). Considering that one of the main targets of $HCO_3^-$ during sperm capacitation is the atypical adenylyl cyclase ADCY10, we then evaluated whether cAMP and PKA were involved in LIMK1 activation. When PKA was inhibited by addition of the specific inhibitor H89, pLIMK1 was not detected. In addition, when sperm were incubated under non-capacitating conditions but in the presence of dbcAMP and IBMX, pLIMK1 was restored (Fig. 3C). As a control, these experimental conditions were evaluated by assessing the level of proteins phosphorylated on tyrosine residues, which depends on the activation of PKA (Fig. 3D). Altogether, these results demonstrate that activation of PKA is essential for LIMK1 phosphorylation.

To test which of the small GTPases were directly involved in the activation of LIMK1 we used specific inhibitors of Rho/ROCK1 and Rac/PAK1 signaling pathways. None of the inhibitors used in these studies impaired the viability of the cells during the incubation (not shown). In the presence of esterified C4 (a specific Rho GTPases inhibitor) as well as with Y27132 (a specific ROCK1 kinase inhibitor), we observed reduced levels of pLIMK1 in a dose dependent manner (Fig. 4A). In the presence of a specific inhibitor of Rac1 (CAS1177865-17-6), reduced levels of pLIMK1 were also observed. However, no differences were observed when a specific inhibitor of PAK1 (IPA-3) was used (Fig. 4B). These results suggest that both RhoA/C and Rac1 participate in the phosphorylation of LIMK1 through activation of ROCK1 but not PAK1.

Because the activation of PKA is essential for the phosphorylation of LIMK1 and it was also demonstrated that both Rho and Rac are involved in the signaling cascade leading to LIMK1 phosphorylation, we aimed to evaluate the order in which each of these events occur. Thus, sperm were incubated under capacitating conditions in the presence of dbcAMP/IBMX and/or inhibitors of Rho and Rac. The results are shown in Fig. 4C. Addition of dbcAMP increased the levels of pLIMK1. The addition of both, Rho (C4) and Rac inhibitors (CAS1177865-17-6) blocked phosphorylation of LIMK1 in controls as well as in those sperm treated also with dbcAMP and IBMX. Interestingly, addition of dbcAMP increased the levels of pLIMK1 when each of these inhibitors was used separately (Fig. 4D) suggesting that Rho and Rac effects on LIMK1 phosphorylation were occurring by two independent signaling pathways.

Altogether these experiments suggest that the phosphorylation of LIMK1 depends on a cAMP-dependent and Rac/Rho signaling pathway. Furthermore, this hypothesis is also consistent with experiments indicating that sperm incubated under capacitating condition in the presence of dbcAMP/IBMX and H89, the level of pLIMK1 was also inhibited to similar levels to the ones observed when the inhibitors of Rho and Rac were present.

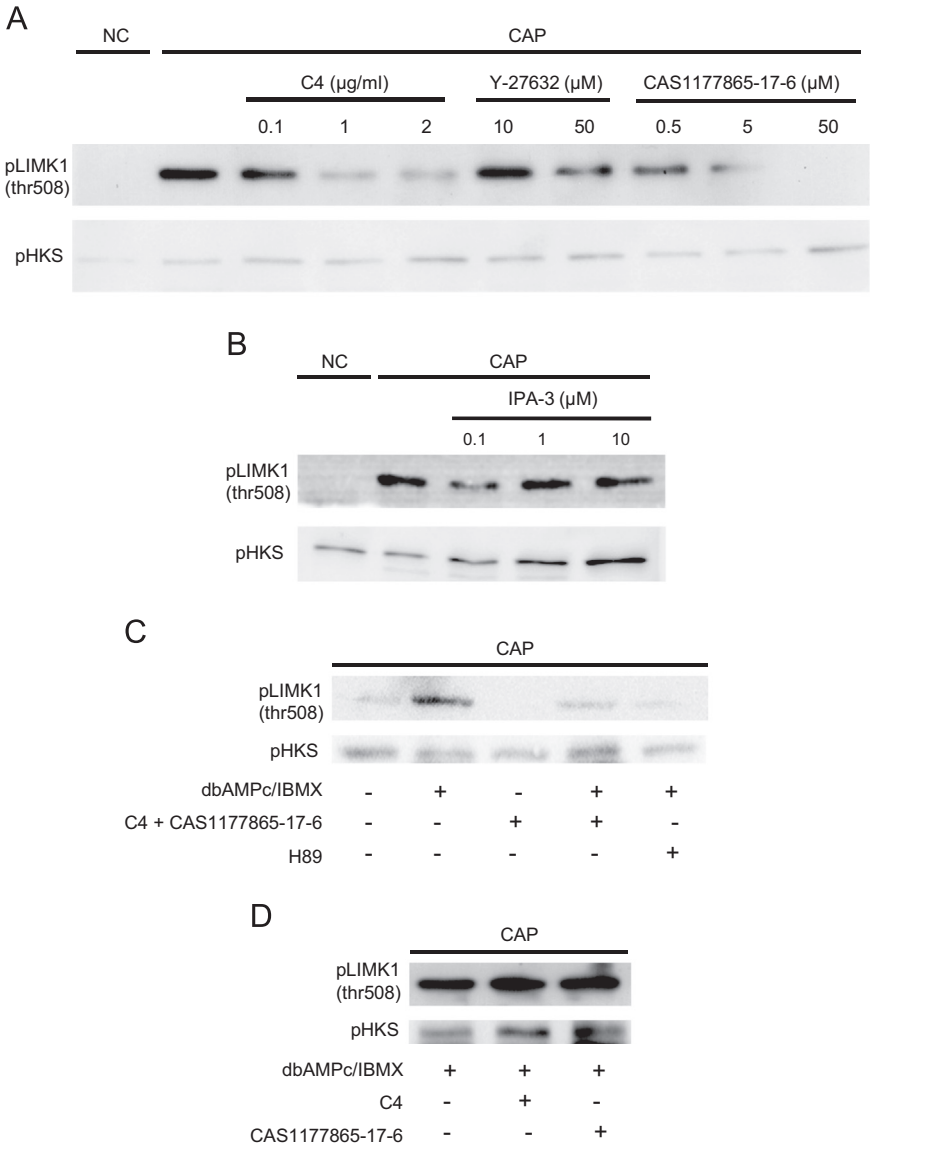


**Fig. 4.** *Inhibition of RHO/ROCK1 and RAC using specific inhibitors decrease the levels of pLIMK1 (Thr508).* Mouse sperm were incubated under capacitating (CAP) and non-capacitating (NC) conditions for 90 min. The Triton-insoluble (I) content of the protein extracts were analyzed by 10% SDS-PAGE and immunoblotted with anti-phospho-LIMK1/2 (Thr508/505) antibody. Each lane contained $5 \times 10^6$ sperm. (A) Sperm were incubated in the presence or absence of increasing concentrations of RHO inhibitor (C4), ROCK1 inhibitor (Y27632) and RAC inhibitor (CAS1177865-17-6). (B) Sperm were incubated in the presence or absence of increasing concentrations of PAK1 inhibitor (IPA-3). (C) Sperm were incubated under capacitating conditions in the presence or absence of both CAS1177865-17-6 (50 μM) and C4 (2 μg/ml), dbAMPc/IBMX (1 mM and 0.2 mM, respectively) and H89 (30 μM). (D) Sperm were incubated under capacitating conditions in the presence of CAS1177865-17-6 (50 μM) or C4 (2 μg/ml) and dbAMPc/IBMX (1 mM and 0.2 mM, respectively). As a loading control, phosphoHexokinase (pHKS) (constitutively phosphorylated on tyrosine) was used. DMSO was used as a vehicle control in CAP and NC. Representative images of 5 independent experiments.

### *3.5. Ser3 of Cofilin is phosphorylated by LIMK1 during capacitation*

Once LIMK1 is phosphorylated, it becomes activated and subsequently phosphorylates Cofilin on Ser3. Depending on the phosphorylation status of Cofilin, it promotes actin polymerization or F-actin cleavage. As shown in Fig. 5A and B, it was observed that during mouse sperm capacitation, Cofilin was phosphorylated on Ser3 (pCofilin) in a transient manner, reaching a maximum at 10 min and then, decreasing to basal levels at approximately 30 min.

Next, we evaluated the distribution of pCofilin and total Cofilin in the Triton X100 soluble and insoluble fractions. Cofilin was distributed in both, the Triton soluble and insoluble fractions. In contrast, pCofilin was mainly observed in the soluble fraction (Fig. 5C). This is in accordance with previous reports that demonstrated pCofilin does not bind to actin filaments (Ghosh et al., 2004; Meberg and Bamburg, 2000; Song et al., 2006).

When sperm were incubated under non-capacitating conditions for 10 min, the levels of pCofilin were lower than cells incubated under capacitating conditions (Fig. 5D). Similarly, the levels of pCofilin were decrease in sperm that were incubated under capacitating conditions for 10 min in the presence of 30 μM of H89, a PKA inhibitor. In contrast, when sperm were incubated under non-capacitating conditions but in the presence of dbcAMP and IBMX, the phosphorylation was restored (Fig. 5D). Altogether, these results suggest that phosphorylation of Cofilin occurs downstream the activation of the cAMP/PKA signaling pathway.

Next, the localization of Cofilin and its phosphorylated form in mouse sperm was evaluated by immunofluorescence. Cofilin was localized in the middle piece and the sperm head. Likewise, pCofilin displayed a similar localization after 10 min of incubation in

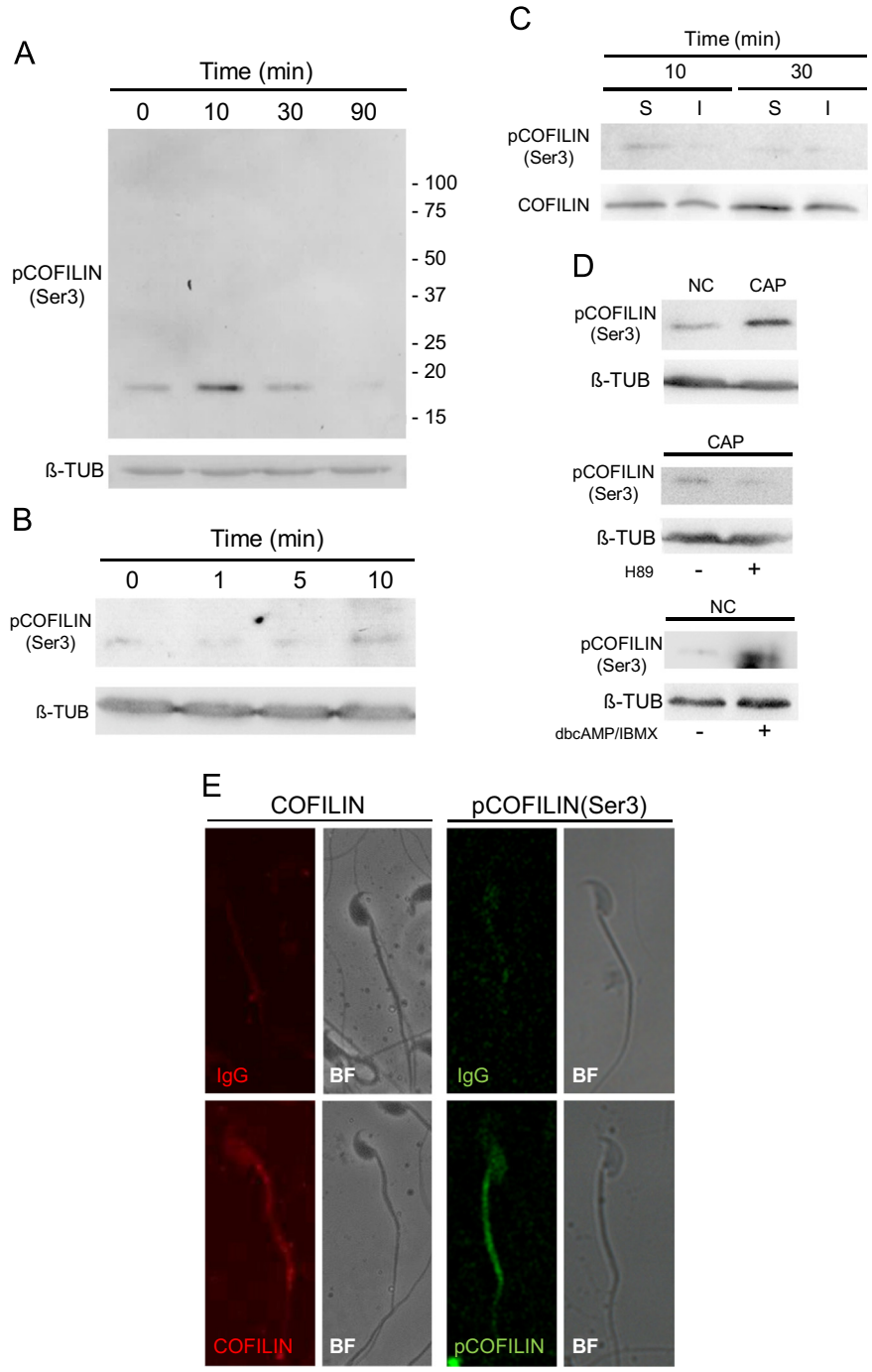


**Fig. 5.** *COFILIN is phosphorylated on Ser3 during capacitation.* Mouse sperm were incubated for different times under capacitating conditions. At the indicated times, the extracted proteins were separated and analyzed by 15% SDS-PAGE and immunoblotted with anti-phosphoCOFILIN (Ser3) antibody. Each lane contained $5 \times 106$ sperm. As a loading control, anti-beta Tubulin (β-TUB) was used. (A and B): The level of phosphorylated COFILIN on Ser3 increased transiently (within 10 min of incubation and decreases after 30 min). (C) Mouse sperm were incubated for 10 and 30 min under capacitating conditions. The Triton-soluble (S) and Triton-insoluble (I) content of the protein extract were analyzed by 15% SDS-PAGE and immunoblotted with anti-phosphoCOFILIN (Ser3) antibody. Each lane contains $5 \times 10^6$ sperm. As a loading control, anti-beta Tubulin was used. (D) Sperm were incubated under capacitating (CAP) or non-capacitating (NC) conditions for 10 min in the presence or absence of dbAMPc/IBMX (1 mM and 0.2 mM, respectively) and H89 (30 μM). The protein extract were analyzed by 15% SDS-PAGE and immunoblotted with anti-phosphoCOFILIN (Ser3) antibody. Each lane contains $5 \times 10^6$ sperm. As a loading control, anti-beta Tubulin was used. (E) Immunofluorescence showing the localization of COFILIN and pCOFILIN (Ser3) in the sperm middle piece and the head after 10 min of incubation in capacitating conditions. BF: bright field images. Negative control was performed incubating the sperm with IgG. Representative images of 5 independent experiments.

capacitating conditions (Fig. 5E).

### *3.6. Inhibition of LIMK1 decreased the phosphorylation of Cofilin and resulted in lower levels of actin polymerization during capacitation*

To demonstrate the direct participation of LIMK1 in the phosphorylation of Cofilin, we used a specific inhibitor of the active form of LIMK1 (BMS-3). Inhibition of pLIMK with 1–50 μM of BMS-3 resulted in a dose-dependent decrease of pCofilin after 10 min incubation in capacitating conditions. As a control, sperm were also incubated for 10 min under non-capacitating conditions which resulted in low levels of pCofilin (Fig. 6).

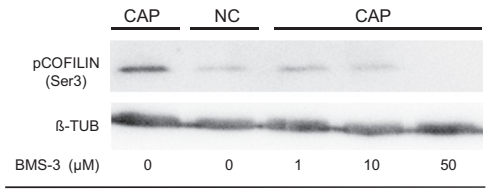


**Fig. 6.** *Inhibition of the active form of LIMK1 with a specific inhibitor results in a decrease of phosphorylated COFILIN on Ser3*. Mouse sperm were incubated under capacitating (CAP) and non-capacitating (NC) conditions for 10 min in the presence or absence of pLIMK inhibitor (BMS-3, 1–50 μM). The protein extract was analyzed by 15% SDS-PAGE and immunoblotted with anti-phosphoCOFILIN (Ser3). As a loading control, anti-β-Tubulin was used. Representative images of 5 independent experiments.

We next decided to evaluate if the specific inhibition of pLIMK would affect the levels of capacitation-induced actin polymerization. Sperm were incubated for 60 min under capacitating conditions based on the time course experiment previously described (see Fig. 1D) where spermatozoa displayed the highest levels of actin polymerization. In the presence of 1 or 50 μM of BMS-3, actin polymerization levels were significantly lower compared to controls (DMSO), suggesting a direct participation of LIMK1 and Cofilin signaling pathway in the actin polymerization process (Fig. 7A). The lower levels of F-actin were observed both in the tail and in the head of the sperm (Fig. 7B).

### *3.7. Activation of LIMK1/Cofilin is essential for mouse sperm acrosomal exocytosis*

To investigate the role of LIMK1/Cofilin signaling pathway in the process of acrosomal exocytosis, we used transgenic sperm expressing EGFP in their acrosomes and analyzed these cells by flow cytometry. As shown in Fig. 7C, increasing concentrations of BMS-3 resulted in a strong decrease on the percentage of sperm that underwent acrosomal exocytosis after stimulation with 20 μM of progesterone. This inhibition was also observed when the acrosomal exocytosis was induced with 50 μM of progesterone or with the stimulation with 10 μM of calcium ionophore A23187 (Fig. 7D). In Fig. 7E–G are shown the representative experiments using flow cytometry analysis of Acr-EGFP sperm. These results suggest that when pLIMK1 is inhibited, the polymerization of actin is reduced and consequently, a markedly decrease in the number of sperm that are able to undergo acrosomal exocytosis is observed.

## 4. Discussion

During capacitation, sperm acquire the ability to undergo acrosomal exocytosis which is an essential step for fertilization. At the molecular level, capacitation is associated with numerous changes that are important for exocytosis including the capacitation-induced actin polymerization (Buffone et al., 2012, 2014). The polymerization of actin is critical in controlling the processes of exocytosis in somatic cells. In sperm, both actin depolymerization and membrane fusion depends on relatively high calcium concentrations which support the concept that actin filaments constitute the final barrier to fusion (Finkelstein et al., 2010; Spungin et al., 1995). Thus, understanding how the dynamics of the actin cytoskeleton are controlled during this process is critical.

Previous reports have postulated that actin is polymerized during sperm capacitation in several species (Brener et al., 2003). Moreover, it has been proposed that this process depends on phospholipase D (PLD) (Cohen et al., 2004) whose activity is regulated by the crosstalk between PKA and PKC and by the activation of phosphatidylinositol 4-kinase (PI4K). It has been postulated that when sperm are stimulated by progesterone or ZP, the F-actin network must be disassembled to allow sperm to undergo exocytosis, and the protein Gelsolin may play a critical role in that step (Finkelstein et al., 2010).

In other cell systems, a group of proteins belonging to the family of small Rho GTPases are known to be involved in controlling actin dynamics. Mammalian Rho GTPases comprise a family of intracellular signaling molecules, best documented for their important roles in regulating the actin cytoskeleton (Heasman and Ridley, 2008). Most studies have focused on the classically activated Rho GTPases, such as RhoA, Rac1 and Cdc42. Their specific function in mammalian sperm remains largely unknown due to the embryonic lethality observed when any of these proteins is targeted deleted (Heasman and Ridley, 2008) and the lack of a sperm-specific conditional mouse. We found that most of these proteins as well as the effector proteins that function downstream their activation are expressed in mouse sperm. In particular, the activation of Rho, Rac1 or Cdc42 leads to the activation of LIMK1/2. In other systems, LIMK can integrate signals from a number of upstream pathways in regulating the actin cytoskeleton (Scott and Olson, 2007). In the testis, LIMK1 is expressed in all the cells while LIMK2 is found only in the elongated spermatids, suggesting that LIMK1 and LIMK2 have cell-specific functions (Acevedo et al., 2006). In addition, LIMK2 is expressed as a testis-specific isoform (Takahashi et al., 2002).

We observed that mouse sperm expressed both LIMK1 and LIMK2 at the expected molecular weights. Similar to many other kinases, phosphorylation in the activation loop results in increased LIMK activity. Both LIMK1 and LIMK2 are phosphorylated on conserved threonine residues (Thr508 in LIMK1 and Thr505 in LIMK2) by the Rho effector Rho kinase (ROCK) and through p21-activated kinase (PAK)1 and PAK4 (by Rac/Cdc42) and these phosphorylation events are required for LIMK activation (Scott and Olson, 2007).

We observed for the first time that LIMK1 is phosphorylated during mouse sperm capacitation. The phosphorylated kinase displayed a molecular weight of 72,000 $M_r$, suggesting that LIMK1 and not LIMK2 is phosphorylated on Thr508. Increased levels of pLIMK were detected as early as 15 min in capacitating conditions and strongly depended on the activation of the cAMP/PKA signaling pathway. A growing literature suggests that actin cytoskeletal dynamics utilize PKA to modulate adhesion-associated events (Howe, 2004). In addition, while some events of cytoskeletal organization require PKA activity (e.g. activation of Rac1 and Cdc42; actin filament assembly), others are inhibited by it (e.g. activation of RhoA). RhoA can be directly phosphorylated by PKA at Ser188 near its C-terminus, and this modification may inhibit its activity (Dong et al., 1998). This possibilities need to be assessed in mouse sperm.

When we used specific inhibitors for Rho/ROCK signaling pathway, we observed a dose-dependent decrease in the levels of pLIMK1. Inhibition of Rac1 also resulted in decreased levels of pLIMK1. However, when PAK1, a kinase that acts downstream the activation of Rac1 and Cdc42, was inhibited, we did not observe any change on the levels of pLIMK1. One possibility is that Rac1 is modulating the levels of pLIMK1 by PAK4 (Soosairajah et al., 2005).

The most extensively characterized substrate of LIMK1 is Cofilin. Members of the ADF/Cofilin family of actin-binding proteins, which are essential in eukaryotes, have long been known to play a key role in actin-filament dynamics in cells and to have interesting modes of regulation. Phosphorylation of Cofilin on Ser3 by activated LIMK is the best characterized way of regulation of this protein. Phosphorylated Cofilin is inactive and no longer binds or severs F-actin (Bamburg and Wiggan, 2002). In this work, we demonstrated that the levels of phosphorylated Cofilin increased

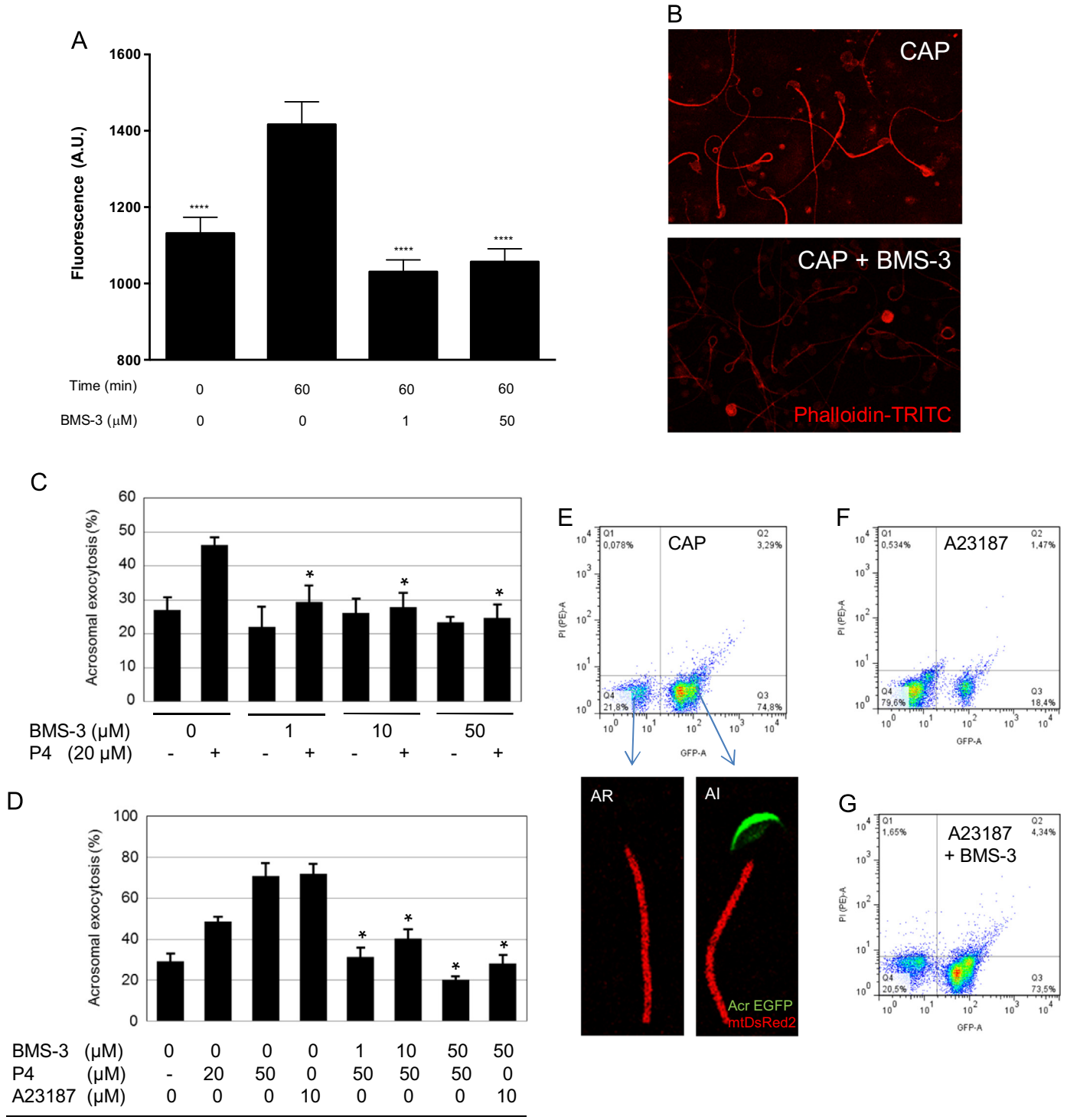


**Fig. 7.** *Inhibition of pLIMK1 produces a decrease in the capacitation-associated actin polymerization and in the percentage of sperm that undergo acrosomal exocytosis upon progesterone or calcium ionophore stimulation.* (A) Mouse spermatozoa were incubated in capacitation conditions in the presence or absence of 1 or 50 μM of BMS-3 and the amount of F-actin in the sperm head was determined after 60 min of incubation. The data represent the mean ± SEM of three experiments; **** represents significant difference compared to 60 min, $P < 0.001$. (B) Representative images from fluorescence microscopy of the fluorescence of F-actin–TRITC-phalloidin. A.U. denotes arbitrary units. (C) and (D) Mouse sperm were incubated under capacitating conditions for 90 min in the presence or absence of increasing concentrations of pLIMK inhibitor BMS-3. After 90 min, progesterone (20 or 50 μM) or calcium ionophore A23187 (10 μM) were added to stimulate acrosomal exocytosis. Acrosomal exocytosis was assessed by flow cytometry analysis of Acr-EGFP sperm. (E–G) Representative experiments using flow cytometry analysis of Acr-EGFP sperm evaluated after capacitation (E), after capacitation in the presence of 10 μM A23187 (F) and after capacitation in the presence of 50 μM BMS-3 and the addition of 10 μM A23187 (G). EGFP-sperm were stained with propidium iodide (PI) to evaluate viability by flow cytometry. Two-dimensional plots differentiated between spermatozoa with low (live) or high (dead) PI staining (*y*-axis) and those with low (acrosome-reacted) or high (intact) EGFP fluorescence (*x*-axis). The lower-right quadrant represents live, acrosome-intact spermatozoa; the upper quadrants represent dead spermatozoa. The lower left quadrant represents live, acrosome-reacted spermatozoa. Cytometric assays were repeated 5 times. The data represent the mean ± SEM of five experiments; * represents significant difference, $P < 0.05$ compared to the same condition without the inhibitor.

transiently during capacitation, reaching a maximum at 10 min of incubation and returning to basal levels after 30 min. Interestingly, pCofilin localized in the Triton-X100 soluble fraction because pCofilin does not bind to detergent-insoluble F-actin. When the active form of LIMK1 was inhibited using specific inhibitors (BMS-3), an increase in pCofilin was not observed suggesting that this protein is phosphorylated by LIMK1.

Proteins regulated by phosphorylation are typically reverted to their basal unphosphorylated state by phosphatases. Two types of Cofilin-selective phosphatases have been identified: the Slingshot family of phosphatases (SSH1) and Chronophin (Niwa et al., 2002). The phosphatase PP2B (Calcineurin) was observed to dephosphorylate and activate SSH1 (Soosairajah et al., 2005). In addition, SSH1 activity was inhibited by PAK4-mediated phosphorylation and possibly others including ROCK and MRCKα (Soosairajah et al., 2005). Other reports demonstrated that SSH1 phosphatase may dephosphorylate and inactivate LIMK1 as well (Soosairajah et al., 2005). These results hamper our understanding of Cofilin regulation because changes in pCofilin levels could be generated by direct SSH1 dephosphorylation, SSH1-mediated LIMK inactivation, or a combination of both.

To understand the physiological implication of inhibiting the LIMK/Cofilin signaling pathway in sperm physiology, we demonstrated that inhibition of pLIMK1 with BMS-3 resulted in low levels of F-actin. What is the relative contribution of RhoA/C and Rac1 during capacitation is still unknown. Another important aspect to determine is how the LIMK1/Cofilin signaling pathway interacts with PLD1, which was shown to be essential for actin polymerization in bovine sperm. One interesting possibility is that pCofilin stimulates PLD1 activity as demonstrated recently (Han et al., 2007).

Acrosomal exocytosis was completely abolished in the presence of the inhibitor of the active form of LIMK1 when stimulated with low or high concentrations of progesterone as well as with calcium ionophore. Although the simplest hypothesis is that the reduced levels of actin polymerization altered some of the critical events leading to exocytosis such as membrane docking, tethering or fusion itself, other possible unknown LIMK targets that function

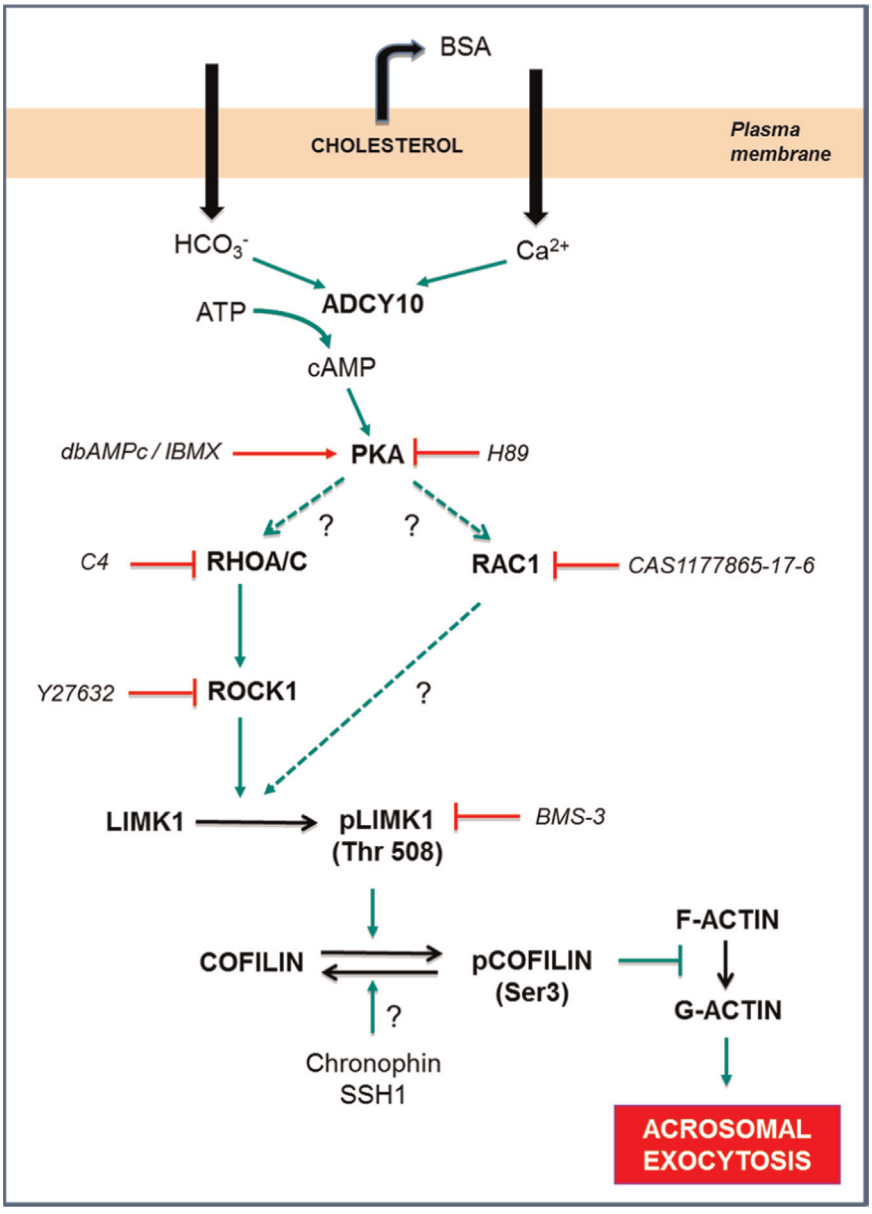


**Fig. 8.** Working model of the sequence of events involved in the participation of the small GTPases in the preparation of spermatozoa for the acrosome reaction. The details are explained in Section 4.

downstream its activation may be also important for the process; however, this possibility needs to be determined.

Thus, we demonstrated for the first time that the master regulators of actin dynamics in somatic cells are present and active in mouse sperm. Combining the results of our present study with other results from the literature, we have proposed a working model regarding how LIMK1/Cofilin controls acrosomal exocytosis in mouse sperm (Fig. 8). During capacitation, the cholesterol efflux leads to a rapid activation of ADCY10 by $HCO_3^-$ and calcium, which results in increased levels of cAMP which in turn, activates PKA. These rapid events promote the activation of RhoA/C and Rac1. RhoA/C activates ROCK1 which in turn phosphorylate LIMK1 on Thr508. Rac1 activation leads to LIMK1 phosphorylation by PAK kinases (possibly through PAK4). Activation of LIMK1 promotes the transient phosphorylation of Cofilin on Ser3, which no longer binds and severs F-actin. The levels of pCofilin may also be modulated by phosphatases such as Chronophin and SSH1. Phosphorylation of Cofilin leads to F-actin polymerization that is essential for acrosomal exocytosis to occur.

## 5. Conclusions

We demonstrated for the first time that the master regulators of actin dynamics in somatic cells are present and active in mouse sperm. During capacitation, the activation of the signaling pathways of cAMP/PKA and the small GTPases RhoA/C and Rac1 are essential for LIMK1 and Cofilin activation by phosphorylation on Threonine 508 and Serine 3 respectively. Inhibition of LIMK1 by specific inhibitors resulted in lower levels of actin polymerization during capacitation and a dramatic decrease in the percentage of sperm that undergo acrosomal exocytosis. Thus, the control of this signaling pathway leading to actin polymerization during sperm capacitation would be an essential step for preparing the sperm to undergo exocytosis.

## Disclosures

No conflicts of interest, financial or otherwise, are declared by the authors.

## Acknowledgments

We would like to thank Dr. George L. Gerton, Dr. Alberto Darszon and Vanina Da Ross for their insightful comments. We also would like to thank Dr. Rafael Baltiérrez-Hoyos and Monica Vazquez for their technical assistance. This work was supported by the National Institutes of Health (RO1TW008662 to MGB), the Eunice Kennedy Shriver National Institute of Child Health and Human Development, NIH (RO1 HD38082 and HD44044 to P.E.V), World Health Organization RMG Grant (H9/TSA/037 to PSC), Agencia Nacional de Promoción Cientifica y Tecnológica (PICT 2013-1175 to MGB, PICT 2011–0540 to DK and PICT 2012–2023 to PSC) and CONICET (PIP 740 to MGB and DK and PIP 290 to PSC).

## References

Austin, C.R., 1951. Observations on the penetration of the sperm in the mammalian egg. Aust. J. Sci. Res. Ser. B Biol. Sci. 4, 581–596.

Amano, T., Tanabe, K., Eto, T., Narumiya, S., Mizuno, K., 2001. LIM-kinase 2 induces formation of stress fibres, focal adhesions and membrane blebs, dependent on its activation by Rho-associated kinase-catalysed phosphorylation at threonine-505. Biochem. J. 354, 149–159.

Acevedo, K., Moussi, N., Li, R., Soo, P., Bernard, O., 2006. LIM kinase 2 is widely expressed in all tissues. J. Histochem. Cytochem.: Off. J. Histochem. Soc 54, 487–501. http://dx.doi.org/10.1369/jhc.5C6813.2006.

Buffone, M.G., Rodriguez-Miranda, E., Storey, B.T., Gerton, G.L., 2009. Acrosomal exocytosis of mouse sperm progresses in a consistent direction in response to zona pellucida. J. Cell. Physiol. 220, 611–620. http://dx.doi.org/10.1002/jcp.21781.

Brener, E., Rubinstein, S., Cohen, G., Shternall, K., Rivlin, J., Breitbart, H., 2003. Remodeling of the actin cytoskeleton during mammalian sperm capacitation and acrosome reaction. Biol. Reprod. 68, 837–845.

Baltiérrez-Hoyos, R., Roa-Espitia, A.L., Hernández-González, E.O., 2012. The association between CDC42 and caveolin-1 is involved in the regulation of capacitation and acrosome reaction of guinea pig and mouse sperm. Reproduction 144, 123–134. http://dx.doi.org/10.1530/REP-11-0433.

Bernstein, B.W., Bamburg, J.R., 2010. ADF/cofilin: a functional node in cell biology. Trends Cell Biol. 20, 187–195. http://dx.doi.org/10.1016/j.tcb.2010.01.001.

Buffone, M.G., Ijiri, T.W., Cao, W., Merdiushev, T., Aghajanian, H.K., Gerton, G.L., 2012. Heads or tails? structural events and molecular mechanisms that promote mammalian sperm acrosomal exocytosis and motility. Mol. Reprod. Dev. 79, 4–18. http://dx.doi.org/10.1002/mrd.21393.

Buffone, M.G., Hirohashi, N., Gerton, G.L., 2014. Unresolved questions concerning mammalian sperm acrosomal exocytosis. Biol. Reprod. 90, 112. http://dx.doi.org/10.1095/biolreprod.114.117911.

Bamburg, J.R., Wiggan, O.P., 2002. ADF/cofilin and actin dynamics in disease. Trends Cell Biol. 12, 598–605.

Chang, M.C., 1951. Fertilizing capacity of spermatozoa deposited into the fallopian tubes. Nature 168, 697–698.

Cabello-Agüeros, J.F., Hernández-González, E.O., Mújica, A., 2003. The role of F-actin cytoskeleton-associated gelsolin in the guinea pig capacitation and acrosome reaction. Cell Motil. Cytoskelet. 56, 94–108. http://dx.doi.org/10.1002/cm.10135.

Cohen, G., Rubinstein, S., Gur, Y., Breitbart, H., 2004. Crosstalk between protein kinase A and C regulates phospholipase D and F-actin formation during sperm capacitation. Dev. Biol. 267, 230–241. http://dx.doi.org/10.1016/j.ydbio.2003.10.034.

Dam, A.H.D.M., Feenstra, I., Westphal, J.R., Ramos, L., van Golde, R.J.T., Kremer, J. a M., 2007. Globozoospermia revisited. Hum. Reprod. Update 13, 63–75. http://dx.doi.org/10.1093/humupd/dml047.

De Blas, G.A., Roggero, C.M., Tomes, C.N., Mayorga, L.S., 2005. Dynamics of SNARE assembly and disassembly during sperm acrosomal exocytosis. PLoS Biol. 3, e323. http://dx.doi.org/10.1371/journal.pbio.0030323.

De La Vega-Beltran, J.L., Sánchez-Cárdenas, C., Krapf, D., Hernandez-González, E.O., Wertheimer, E., Treviño, C.L., et al., 2012. Mouse sperm membrane potential hyperpolarization is necessary and sufficient to prepare sperm for the acrosome reaction. J. Biol. Chem. 287, 44384–44393. http://dx.doi.org/10.1074/jbc.M112.393488.

Ducummon, C.C., Berger, T., 2006. Localization of the Rho GTPases and some Rho effector proteins in the sperm of several mammalian species. Zygote 14, 249–257. http://dx.doi.org/10.1017/S0967199406003790.

Delgado-Buenrostro, N.L., Hernández-González, E.O., Segura-Nieto, M., Mújica, A., 2005. Actin polymerization in the equatorial and postacrosomal regions of guinea pig spermatozoa during the acrosome reaction is regulated by G proteins. Mol. Reprod. Dev. 70, 198–210. http://dx.doi.org/10.1002/mrd.20192.

Dong, J.M., Leung, T., Manser, E., Lim, L., 1998. cAMP-induced morphological changes are counteracted by the activated RhoA small GTPase and the Rho kinase ROKalpha. J. Biol. Chem. 273, 22554–22562.

Finkelstein, M., Etkovitz, N., Breitbart, H., 2010. Role and regulation of sperm gelsolin prior to fertilization. J. Biol. Chem. 285, 39702–39709. http://dx.doi.org/10.1074/jbc.M110.170951.

Fiedler, S.E., Bajpai, M., Carr, D.W., 2008. Identification and characterization of RHOA-interacting proteins in bovine spermatozoa. Biol. Reprod. 78, 184–192. http://dx.doi.org/10.1095/biolreprod.107.062943.

Freeman, E.A., Jani, P., Millette, C.E., 2002. Expression and potential function of Rho family small G proteins in cells of the mammalian seminiferous epithelium. Cell Commun. Adhes. 9, 189–204.

Ghosh, M., Song, X., Mouneimne, G., Sidani, M., Lawrence, D.S., Condeelis, J.S., 2004. Cofilin promotes actin polymerization and defines the direction of cell motility. Science 304, 743–746. http://dx.doi.org/10.1126/science.1094561.

Hutt, D.M., Baltz, J.M., Ngsee, J.K., 2005. Synaptotagmin VI and VIII and syntaxin 2 are essential for the mouse sperm acrosome reaction. J. Biol. Chem. 280, 20197–20203. http://dx.doi.org/10.1074/jbc.M412920200.

Hernández-González, E.O., Lecona-Valera, A.N., Escobar-Herrera, J., Mújica, A., 2000. Involvement of an F-actin skeleton on the acrosome reaction in guinea pig spermatozoa. Cell Motil. Cytoskelet. 46, 43–58. http://dx.doi.org/10.1002/(SICI)1097 0169(200005)46:1 < 43::AID-CM5 > 3.0.CO;2-1.

Hasuwa, H., Muro, Y., Ikawa, M., Kato, N., Tsujimoto, Y., Okabe, M., 2010. Transgenic mouse sperm that have green acrosome and red mitochondria allow visualization of sperm and their acrosome reaction in vivo. Exp. Anim. Jpn. Assoc. Lab. Anim. Sci. 59, 105–107.

Hirohashi, N., Spina, F.A.L., Romarowski, A., Buffone, M.G., 2015. Redistribution of the intra-acrosomal EGFP before acrosomal exocytosis in mouse spermatozoa. Reproduction 149, 657–663. http://dx.doi.org/10.1530/REP-15-0017.

Heasman, S.J., Ridley, A.J., 2008. Mammalian Rho GTPases: new insights into their functions from in vivo studies. Nat. Rev. Mol. Cell Biol. 9, 690–701. http://dx.doi.org/10.1038/nrm2476.

Howe, A.K., 2004. Regulation of actin-based cell migration by cAMP/PKA. Biochim. Biophys. Acta 1692, 159–174. http://dx.doi.org/10.1016/j.bbamcr.2004.03.005.

Han, L., Stope, M.B., de Jesús, M.L., Oude Weernink, P.A., Urban, M., Wieland, T.,

et al., 2007. Direct stimulation of receptor-controlled phospholipase D1 by phospho-cofilin. EMBO J. 26, 4189–4202. http://dx.doi.org/10.1038/sj.emboj.7601852.
Itach, S.B.-S., Finklestein, M., Etkovitz, N., Breitbart, H., 2012. Hyper-activated motility in sperm capacitation is mediated by phospholipase D-dependent actin polymerization. Dev. Biol. 362, 154–161. http://dx.doi.org/10.1016/j.ydbio.2011.12.002.
Kang-Decker, N., Mantchev, G.T., Juneja, S.C., McNiven, M.A., van Deursen, J.M., 2001. Lack of acrosome formation in Hrb-deficient mice. Science 294, 1531–1533. http://dx.doi.org/10.1126/science.1063665.
Kalab, P., Visconti, P., Leclerc, P., Kopf, G.S., 1994. p95, the major phosphotyrosine-containing protein in mouse spermatozoa, is a hexokinase with unique properties. J. Biol. Chem. 269, 3810–3817.
Lin, Y.-N., Roy, A., Yan, W., Burns, K.H., Matzuk, M.M., 2007. Loss of zona pellucida binding proteins in the acrosomal matrix disrupts acrosome biogenesis and sperm morphogenesis. Mol. Cell. Biol. 27, 6794–6805. http://dx.doi.org/10.1128/MCB.01029-07.
Laemmli, U.K., 1970. Cleavage of structural proteins during the assembly of the head of bacteriophage T4. Nature 227, 680–685.
Miranda, P.V., Allaire, A., Sosnik, J., Visconti, P.E., 2009. Localization of low-density detergent-resistant membrane proteins in intact and acrosome-reacted mouse sperm. Biol. Reprod. 80, 897–904. http://dx.doi.org/10.1095/biolreprod.108.075242.
Mayorga, L.S., Tomes, C.N., Belmonte, S.A., 2007. Acrosomal exocytosis, a special type of regulated secretion. IUBMB Life 59, 286–292. http://dx.doi.org/10.1080/15216540701222872.
Michaut, M., De Blas, G., Tomes, C.N., Yunes, R., Fukuda, M., Mayorga, L.S., 2001. Synaptotagmin VI participates in the acrosome reaction of human spermatozoa. Dev. Biol. 235, 521–529. http://dx.doi.org/10.1006/dbio.2001.0316.
Muallem, S., Kwiatkowska, K., Xu, X., Yin, H.L., 1995. Actin filament disassembly is a sufficient final trigger for exocytosis in nonexcitable cells. J. Cell Biol. 128, 589–598.
Moore, G.D., Ayabe, T., Visconti, P.E., Schultz, R.M., Kopf, G.S., 1994. Roles of heterotrimeric and monomeric G proteins in sperm-induced activation of mouse eggs. Development 120, 3313–3323.
Muro, Y., Buffone, M.G., Okabe, M., Gerton, G.L., 2012. Function of the acrosomal matrix: zona pellucida 3 receptor (ZP3R/sp56) is not essential for mouse fertilization. Biol. Reprod. 86, 1–6. http://dx.doi.org/10.1095/biolreprod.111.095877.
Meberg, P.J., Bamburg, J.R., 2000. Increase in neurite outgrowth mediated by overexpression of actin depolymerizing factor. J. Neurosci.: Off. J. Soc. Neurosci. 20, 2459–2469.
Nemoto, T., Kojima, T., Oshima, A., Bito, H., Kasai, H., 2004. Stabilization of exocytosis by dynamic F-actin coating of zymogen granules in pancreatic acini. J. Biol. Chem. 279, 37544–37550. http://dx.doi.org/10.1074/jbc.M403976200.
Niwa, R., Nagata-Ohashi, K., Takeichi, M., Mizuno, K., Uemura, T., 2002. Control of actin reorganization by Slingshot, a family of phosphatases that dephosphorylate ADF/cofilin. Cell 108, 233–246.
Ohashi, K., Nagata, K., Maekawa, M., Ishizaki, T., Narumiya, S., Mizuno, K., 2000. Rho-associated kinase ROCK activates LIM-kinase 1 by phosphorylation at threonine 508 within the activation loop. J. Biol. Chem. 275, 3577–3582.
Porat-Shliom, N., Milberg, O., Masedunskas, A., Weigert, R., 2013. Multiple roles for the actin cytoskeleton during regulated exocytosis. Cell. Mol. Life Sci.: CMLS 70, 2099–2121. http://dx.doi.org/10.1007/s00018-012-1156-5.
Rodríguez, F., Bustos, M.A., Zanetti, M.N., Ruete, M.C., Mayorga, L.S., Tomes, C.N., 2011. α-SNAP prevents docking of the acrosome during sperm exocytosis because it sequesters monomeric syntaxin. PLoS One 6, e21925. http://dx.doi.org/10.1371/journal.pone.0021925.
Roggero, C.M., De Blas, G.A., Dai, H., Tomes, C.N., Rizo, J., Mayorga, L.S., 2007. Complexin/synaptotagmin interplay controls acrosomal exocytosis. J. Biol. Chem. 282, 26335–26343. http://dx.doi.org/10.1074/jbc.M700854200.
Spungin, B., Margalit, I., Breitbart, H., 1995. Sperm exocytosis reconstructed in a cell-free system: evidence for the involvement of phospholipase C and actin filaments in membrane fusion. J. Cell Sci. 108 (Pt 6), 2525–2535.
Sosnik, J., Buffone, M.G., Visconti, P.E., 2010. Analysis of CAPZA3 localization reveals temporally discrete events during the acrosome reaction. J. Cell. Physiol. 224, 575–580. http://dx.doi.org/10.1002/jcp.22211.
Song, X., Chen, X., Yamaguchi, H., Mouneimne, G., Condeelis, J.S., Eddy, R.J., 2006. Initiation of cofilin activity in response to EGF is uncoupled from cofilin phosphorylation and dephosphorylation in carcinoma cells. J. Cell Sci. 119, 2871–2881. http://dx.doi.org/10.1242/jcs.03017.
Scott, R.W., Olson, M.F., 2007. LIM kinases: function, regulation and association with human disease. J. Mol. Med. 85, 555–568. http://dx.doi.org/10.1007/s00109-007-0165-6.
Soosairajah, J., Maiti, S., Wiggan, O., Sarmiere, P., Moussi, N., Sarcevic, B., et al., 2005. Interplay between components of a novel LIM kinase-slingshot phosphatase complex regulates cofilin. EMBO J. 24, 473–486. http://dx.doi.org/10.1038/sj.emboj.7600543.
Tomes, C.N., De Blas, G.A., Michaut, M.A., Farré, E.V., Cherhitin, O., Visconti, P.E., et al., 2005. alpha-SNAP and NSF are required in a priming step during the human sperm acrosome reaction. Mol. Hum. Reprod. 11, 43–51. http://dx.doi.org/10.1093/molehr/gah126.
Towbin, H., Staehelin, T., Gordon, J., 1979. Electrophoretic transfer of proteins from polyacrylamide gels to nitrocellulose sheets: procedure and some applications. Proc. Natl. Acad. Sci. USA 76, 4350–4354.
Takahashi, H., Koshimizu, U., Miyazaki, J., Nakamura, T., 2002. Impaired spermatogenic ability of testicular germ cells in mice deficient in the LIM-kinase 2 gene. Dev. Biol. 241, 259–272. http://dx.doi.org/10.1006/dbio.2001.0512.
Visconti, P.E., Bailey, J.L., Moore, G.D., Pan, D., Olds-Clarke, P., Kopf, G.S., 1995. Capacitation of mouse spermatozoa. I. Correlation between the capacitation state and protein tyrosine phosphorylation. Development 121, 1129–1137.
Yanagimachi, R., 1994. Fertility of mammalian spermatozoa: its development and relativity. Zygote 2, 371–372.
Yunes, R., Tomes, C., Michaut, M., De Blas, G., Rodriguez, F., Regazzi, R., et al., 2002. Rab3A and calmodulin regulate acrosomal exocytosis by mechanisms that do not require a direct interaction. FEBS Lett. 525, 126–130.
Zhao, L., Burkin, H.R., Shi, X., Li, L., Reim, K., Miller, D.J., 2007. Complexin I is required for mammalian sperm acrosomal exocytosis. Dev. Biol. 309, 236–244. http://dx.doi.org/10.1016/j.ydbio.2007.07.009.